JOURNAL OF SOLID STATE CHEMISTRY **132,** 173–181 (1997)
ARTICLE NO. SC977440

Crystal Structure of Tribasic Lead Sulfate ($3PbO \cdot PbSO_4 \cdot H_2O$) by X-Rays and Neutrons: An Intermediate Phase in the Production of Lead Acid Batteries

Ian M. Steele,* Joseph J. Pluth,*,†,‡ and James W. Richardson, Jr.§

* *Department of Geophysical Sciences,* † *Consortium for Advanced Radiation Sources,* ‡ *Materials Research Science and Engineering Center, The University of Chicago, Chicago Illinois 60637; and* § *Intense Pulsed Neutron Source, Argonne National Laboratory, 9700 South Cass Avenue, Argonne, Illinois 60439-4814*

Received March 17, 1997; accepted April 22, 1997

The crystal structure of tribasic lead sulfate ($3PbO \cdot PbSO_4 \cdot H_2O$) has been determined by a combination of single crystal X-ray and powder neutron diffraction to *R* of 0.024. From X-ray data, the space group is $P\bar{1}$, $a = 6.378(1)$, $b = 7.454(2)$, $c = 10.308(2)$ Å, $\alpha = 75.26(3)$, $\beta = 79.37(3)$, $\gamma = 88.16(3)^\circ$. The structure can be represented with two types of layers: (i) hexagonal nets of Pb and (ii) similar layers but with 1/2 of Pb replaced by equal numbers of S and 2H. These layers are stacked in the sequence ... BAABAA ... Structural units can be identified in tetragonal and orthorhombic PbO which are also present in tribasic lead sulfate and provide a common basis for relating these structures. These units are defined by Pb–O bonds which are less than 2.5 Å which represent the strongest linkages. Two OH groups form weak hydrogen bonds to a single oxygen of a sulfate group. Lead polyhedra show both a range in coordination and Pb–O distances consistent with oxygen forming irregular polyhedra within the more regular cation framework. An alternative formula, $4PbO \cdot H_2SO_4$, may better represent the structure with the suggestion that H_2 and SO_4 groups replace Pb rather than the incorporation of H_2O groups.

INTRODUCTION

Two main lead sulfate phases ($4PbO \cdot PbSO_4$ and $3PbO \cdot PbSO_4 \cdot H_2O$) are formed as intermediate products in the production of lead acid batteries used in automotive and industrial applications and potentially in the electric vehicle market. While these two phases have been recognized for many years, e.g., (1), their crystal structures had not previously been determined and thus their possible influence on the resulting active material is uncertain other than by simple experience. Structural data may allow creative modification of crystal shape or other growth parameters to optimize resulting porosity, strength, and surface area. We have determined the crystal structure for one of these phases, $4PbO \cdot PbSO_4$ (tetrabasic lead sulfate) (2), and here report the structure of tribasic lead sulfate ($3PbO \cdot PbSO_4 \cdot H_2O$) as determined by both single crystal X-ray and powder neutron diffraction techniques on two different samples.

The solution of these two lead sulfate structures provides the necessary structural data for Rietveld refinement of all phases occurring during the various stages of battery production. Structural studies are now possible either using X-rays or neutrons where structural parameters and phase abundance can be monitored either in static or dynamic experiments. The static experiments require sacrificing of batteries but allow both scattering experiments and morphological studies. The dynamic experiments would allow similar scattering studies but by using specially constructed cells, *in situ* measurements can be made using neutrons where various parameters such as charge/discharge rates are controlled. This is especially important because these experiments have not been made for lead acid battery systems which are one candidate for the power systems of zero emission (electric) vehicles.

Because of the span in atomic number in these compounds (H, O, S, Pb) and the high absorption, X-rays have limitations in their study. Thus we have used a combination of single crystal X-ray studies where the structural framework is obtained followed by neutron studies of a powder sample to locate the hydrogen atoms. In practice it is expected that neutrons will be the method of choice as X-rays sample only to a limited depth in these high *Z* materials and this may be nonrepresentative of the main battery active material.

EXPERIMENTAL DETAILS AND STRUCTURE SOLUTION

Two types of $3PbO \cdot PbSO_4 \cdot H_2O$ samples were used in this study with a single crystal sample providing data for direct methods determination of the Pb, S, and O positions

0022-4596/97 $25.00

and a powder sample allowing location of the H positions and subsequent refinement of all atom positions for the powder sample. For single crystal X-ray data collection, crystals were obtained from Dr. H. G. Kuzel who grew both tribasic and tetrabasic lead sulfate together from a hydrothermal solution at moderate pressure in a thermal gradient (3). Crystals were elongated plates but always twinned with the twin plane corresponding to the large plate dimension. Efforts to separate individuals were not always successful because of the plastic nature of the compound. However, we used the best sample obtained in this way for data collection but only after verifying that diffractions were sharp and not multiple.

The crystal (details in Table 1) was mounted on an automated Picker–Krisel four-circle diffractometer with the a axis offset 1° from the ϕ axis. Refinement using 20 diffractions ($30 < 2\theta < 38°$: $\lambda = 0.71069$ Å), each the average of automatic centering of 8 equivalent settings gave the cell parameters (Table 1) consistent with triclinic symmetry. A total of 4272 intensities were collected with the θ–2θ technique, scan speed 2°/min, scan width 1.6–2.0° for range 5–55° 2θ. Merging yielded 2136 intensities ($R_{\text{int}} = 0.036$), all of which were used in refinements: data collection range $h \pm 8$, $k \pm 9$, $l \pm 13$; mean intensity variation of three standard diffractions 3%. An analytical absorption correction was applied to the data using the μ value and crystal dimensions in Table 1. No systematic absences were recognized consistent with the space group $P\bar{1}$. The initial model was derived from the direct methods program in SHELXTL. All Pb and S atoms were included in a least squares refinement using anisotropic temperature factors, and the O positions were located in subsequent difference-Fourier maps.

In the final model, 119 variables were refined: scale factor, extinction parameter, positions for 13 atoms, and anisotropic displacement factors. Neutral scattering factors found internal to SHELXTL were used. The final least-squares refinement minimized all F^2s with σ_{F^2} computed from σI, the square root of [total counts +(2% of total counts)^2], $w = (\sigma_F^2)^{-2}$, $R(F) = 0.024$, $R_w(F^2) = 0.054$, $S = 1.04$; largest shift/e.s.d. ~0.000 for all parameters; maximum and minimum heights on final difference-Fourier map are +2.6 and −1.9 eÅ^{-3}; computer programs: local data reduction, SHELXTL. Final atomic coordinates and displacement parameters are given in Tables 2 and 3, respectively.

The powdered sample used for neutron studies was prepared by Halstab Division of the Hammond Group and consisted of a micrometer-sized powder which was verified to be nearly pure tribasic lead sulfate using standard X-ray diffraction. This powder was placed in a vanadium canister and mounted in the general purpose powder diffractometer (GPPD) (4) at the Intense Pulsed Neutron Source (IPNS), Argonne National Laboratory. Time-of-flight neutron diffraction data were accumulated for 20 h. Data from detector

TABLE 1
Experimental Details and Crystallographic Data for $3PbO \cdot PbSO_4 \cdot H_2O$ for X-Ray Diffraction

(A) Crystal-cell data	
a(Å)	6.378(1)
b(Å)	7.454(2)
c(Å)	10.308(2)
α(°)	75.26(3)
β(°)	79.37(3)
γ(°)	88.16(3)
V(Å^3)	465.79(3)
Space group	$P\bar{1}$
Z	4
Formula	$3PbO \cdot PbSO_4 \cdot H_2O$
D_{calc} (g cm^{-3})	7.065
μ (cm^{-1})	72.30
(B) Intensity measurements	
Crystal size	Tetragonal, $0.14 \times 0.04 \times 0.01$ mm
Diffractometer	Picker, Krisel control
Monochromator	Graphite
Radiation	Mo$K\alpha_1$
Scan type	Θ–2Θ
2Θ range	5.0–55.0
Diffractions measured	4272
Unique diffractions	2136
(C) Refinement of the structure	
R 0.024	$R = \sum(\lvert\lvert F_o\rvert - \lvert F_c\rvert\rvert)/\sum\lvert F_o\rvert$
R_w 0.054	$R_w = [\sum w(\lvert F_o^2\rvert - \lvert F_c^2\rvert)^2/\sum w\lvert F_o^2\rvert^2]^{1/2}$
Variable parameters	119
"Goodness of fit" (GOF)	1.04

TABLE 2
Positional and Isotropic Displacement Parameters for $3PbO \cdot PbSO_4 \cdot H_2O$ by X-Ray Diffraction

Atom	x	y	z	$*U_{\text{eq}}$[a]
Pb (1)	0.22887(4)	−0.38568(4)	0.02890(3)	0.0153(1)
Pb (2)	0.24292(4)	0.11800(4)	0.00669(3)	0.0165(1)
Pb (3)	−0.22148(5)	−0.48306(4)	0.32200(3)	0.0201(1)
Pb (4)	−0.18131(6)	0.00098(4)	0.31843(3)	0.0232(1)
S	0.3006(3)	0.2396(3)	0.3250(2)	0.0173(4)
O (1)	0.3968(9)	0.2048(8)	−0.2561(6)	0.0234(13)
O (2)	0.1353(8)	0.4156(7)	−0.0926(6)	0.0143(11)
O (3)	0.0401(9)	−0.2467(9)	0.2703(7)	0.0259(14)
O (4)	−0.1145(8)	0.1008(7)	0.0864(6)	0.0162(11)
O (5)	0.1329(9)	0.3037(9)	0.2403(7)	0.0303(15)
O (6)	−0.4914(9)	0.3015(11)	0.2367(7)	0.0382(18)
O (7)	0.2666(12)	0.3180(10)	0.4427(7)	0.0402(18)
O (8)	0.2905(11)	0.0361(10)	0.3677(7)	0.0356(16)

[a] $*U_{\text{eq}}$ is defined as

$$1/3 \sum_{i=1}^{3} \sum_{j=1}^{3} U_{ij} a_i^* a_j^* (\mathbf{a}_i \cdot \mathbf{a}_j).$$

TABLE 3
Anisotropic Displacement Parameters for $3PbO \cdot PbSO_4 \cdot H_2O$ by X-ray Diffraction

Atom	U_{11}	U_{22}	U_{33}	U_{23}	U_{13}	U_{12}
Pb (1)	0.0144(2)	0.0124(2)	0.0190(2)	− 0.0040(1)	− 0.0028(1)	− 0.0005(1)
Pb (2)	0.0162(2)	0.0140(2)	0.0201(2)	− 0.0053(1)	− 0.0045(1)	0.0018(1)
Pb (3)	0.0275(2)	0.0152(2)	0.0148(2)	− 0.0025(1)	0.0015(1)	− 0.0024(1)
Pb (4)	0.0382(2)	0.0160(2)	0.0138(2)	− 0.0057(1)	0.0028(1)	− 0.0040(1)
S	0.019(1)	0.021(1)	0.012(1)	− 0.005(1)	− 0.001(1)	− 0.001(1)
O (1)	0.026(3)	0.019(3)	0.023(3)	− 0.006(3)	0.002(3)	0.000(2)
O (2)	0.018(3)	0.011(3)	0.013(3)	− 0.006(2)	0.001(2)	− 0.001(2)
O (3)	0.024(3)	0.022(3)	0.031(4)	− 0.005(3)	− 0.003(3)	− 0.005(2)
O (4)	0.019(3)	0.013(3)	0.014(3)	− 0.003(2)	0.002(2)	− 0.001(2)
O (5)	0.021(3)	0.036(4)	0.030(4)	0.001(3)	− 0.007(3)	0.002(3)
O (6)	0.023(3)	0.060(5)	0.027(4)	− 0.004(4)	0.002(3)	− 0.010(3)
O (7)	0.070(5)	0.036(4)	0.016(3)	− 0.016(3)	0.002(3)	− 0.003(4)
O (8)	0.052(4)	0.022(3)	0.028(4)	− 0.001(3)	− 0.003(3)	0.004(3)

banks centered at $2\Theta = \pm 148^\circ$, where a Bragg peak resolution, $\Delta d/d(\mathrm{FWHM}) = 0.25\%$ can be achieved, were used for Rietveld profile refinement (5). A total of 1012 diffractions were present in the *d*-spacing range 1.0–2.8 Å, covering 3937 data points. Starting positional parameters for Pb, S and O atoms were obtained from the X-ray determination. Because the Bragg peaks were quite broad (roughly three times the instrumental resolution) and the symmetry low, the Rietveld refinement was limited to a minimal set of parameters. Refined structural parameters included lattice parameters, fractional coordinates and isotropic Debye–Waller factors for all atoms, and site occupancies for hydrogen atoms, a total of 68 structural parameters. In addition, an overall scale factor, absorption coefficient, and peak shape parameters were refined. The background was fit with a 14-parameter function [available in the GSAS refinement suite (5)] which includes modeling of a diffuse scattering contribution from the sample. A minor phase, $PbO \cdot$

TABLE 4
Experimental Details and Crystallographic Data for $3PbO \cdot PbSO_4 \cdot H_2O$ for Neutron Diffraction

	$3PbO \cdot PbSO_4 \cdot H_2O$	$PbO \cdot PbSO_4$
a(Å)	6.3682(2)	13.7539(12)
b(Å)	7.4539(3)	5.7034(4)
c(Å)	10.2971(4)	7.0746(7)
$\alpha(^\circ)$	75.33(1)	
$\beta(^\circ)$	79.40(1)	115.87(1)
$\gamma(^\circ)$	88.34(1)	
V(Å^3)	464.27(2)	498.82(8)
Absorption coefficient (Å^{-1})	0.27(4)	
Data collection time (hr)	20	
Scattering angle	148°	
d-spacing range (Å)	1.0–2.8	
Diffractions	1012	
Data points	3937	
R_p	0.026	
R_{wp}	0.019	
R_{F^2}	0.032	
Variable parameters	91	
χ^2	1.60	
Vol. fraction (%)	81(3)	19(3)

$R_p = \sum(Y_o - Y_c)/\sum(Y_o)$
$R_{wp} = [\sum w(Y_o^2 - Y_c^2)^2/\sum w(Y_o)^2]^{1/2}$
$R_{F^2} = \sum(I_o - I_c)/\sum(I_o)$

TABLE 5
Positional and Isotropic Displacement Parameters for $3PbO \cdot PbSO_4 \cdot H_2O$ by Neutron Diffraction

Atom	x	y	z	$*U_{eq}$[a]
Pb (1)	0.2307(12)	− 0.3875(11)	0.0262(9)	0.022(3)
Pb (2)	0.2442(16)	0.1182(13)	0.0101(11)	0.051(4)
Pb (3)	− 0.2191(11)	− 0.4803(10)	0.3166(7)	0.025(2)
Pb (4)	− 0.1837(15)	− 0.0025(15)	0.3204(10)	0.052(4)
S	0.295(4)	0.240(3)	0.321(2)	0.018(5)
H(1)	0.449(4)	0.838(3)	0.303(2)	0.04(6)
H(2)	0.162(4)	0.754(3)	0.318(3)	0.05(8)
O (1)	0.391(2)	0.210(2)	− 0.257(1)	0.023(3)
O (2)	0.127(2)	0.414(2)	− 0.089(1)	0.012(3)
O (3)	0.044(3)	− 0.245(2)	0.271(2)	0.056(5)
O (4)	− 0.117(3)	0.080(2)	0.097(2)	0.054(5)
O (5)	0.131(2)	0.296(2)	0.241(2)	0.038(4)
O (6)	− 0.476(3)	0.298(3)	0.240(2)	0.075(6)
O (7)	0.254(2)	0.323(2)	0.441(1)	0.040(3)
O (8)	0.278(2)	0.033(2)	0.375(2)	0.054(4)

[a] $*U_{eq}$ is defined as

$$1/3 \sum_{i=1}^{3} \sum_{j=1}^{3} U_{ij} a_i^* a_j^* (\mathbf{a}_i \cdot \mathbf{a}_j).$$

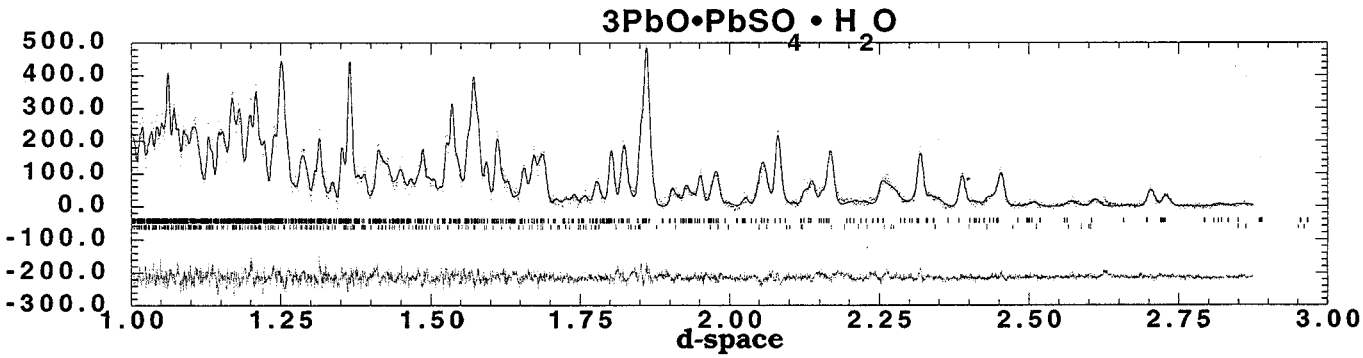

FIG. 1. Observed (dots) vs calculated (solid) neutron diffraction profiles for $3PbO \cdot PbSO_4 \cdot H_2O$ as function of d(Å). Below these two profiles are the calculated peak positions for the main phase and the minor $PbO \cdot PbSO_4$ contaminant phase. At the bottom is the difference plot of observed minus calculated profiles.

$PbSO_4$, was found to be present and its lattice and peak shape parameters were refined, but the positional parameters, taken from (6), were not refined.

Subsequent difference Fourier maps clearly showed the position of the two hydrogen atoms and these were included in subsequent profile refinements. Final lattice, positional, and isotropic thermal parameters are given in Tables 4 and 5, and a comparison of the observed and calculated profiles with residual is shown in Fig. 1. It should be emphasized that the two samples were prepared differently and the difference between X-ray and neutron cell, positional, and thermal parameters may reflect real structural differences.

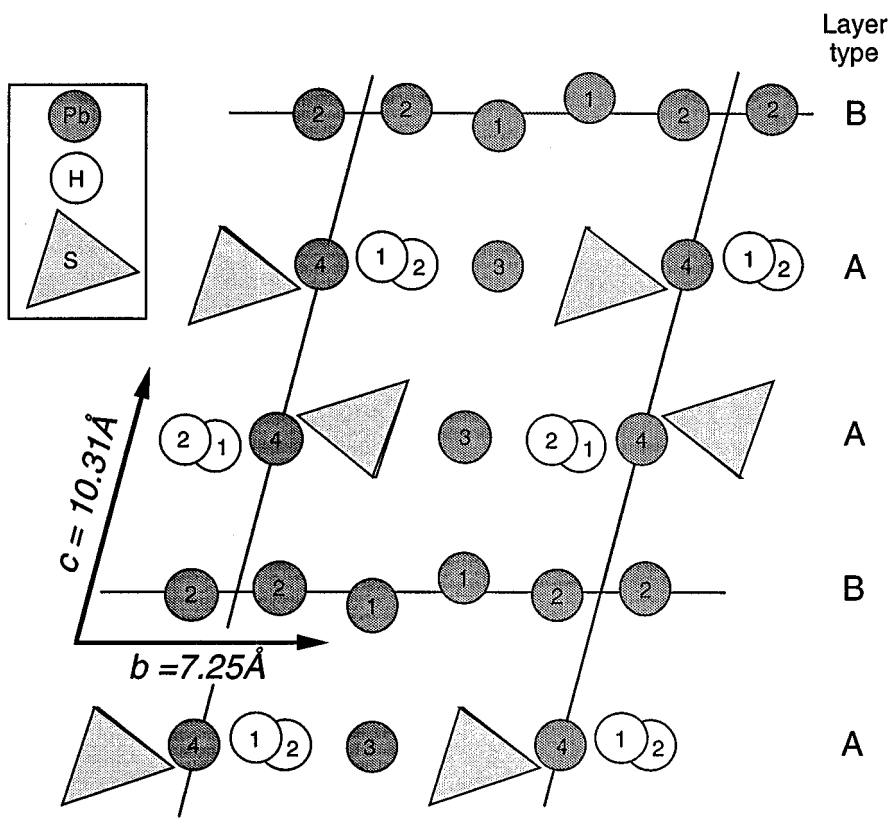

FIG. 2. Projection of cations (Pb, S, H) parallel to [100]. In this view, two types of layers parallel to (001) can be recognized. Layer A is composed of Pb, S, and H while Layer B is composed entirely of Pb. These layers are stacked in the sequence ..BAABAA…

DISCUSSION AND STRUCTURE

Layers, Chains, and Nets

Figure 2 shows a projection in which the cation arrangement appears as alternating layers each parallel to (001) with the stacking sequence ..BAABAA.. The two A layers which are related by a center of symmetry include all S, H, Pb3, and Pb4 while Layer B is composed entirely of Pb1 and Pb2. Both the A and the B layers in turn can be decomposed into chains parallel to the *b* axis formed by edge- and face-sharing PbO_6 and PbO_8 polyhedra in the A layer and PbO_5 and PbO_6 polyhedra for the B layer, respectively. In each case these chains are weakly linked both within and between the layers. The overall cation geometry within each layer can be represented as a hexagonal net. For layer A, 2/3 of the nodes are occupied by Pb and 1/6 each by SO_4 and 2H. For layer B, all nodes are occupied by Pb. These idealized layer nets are illustrated in Fig. 3 and details of each layer are discussed below.

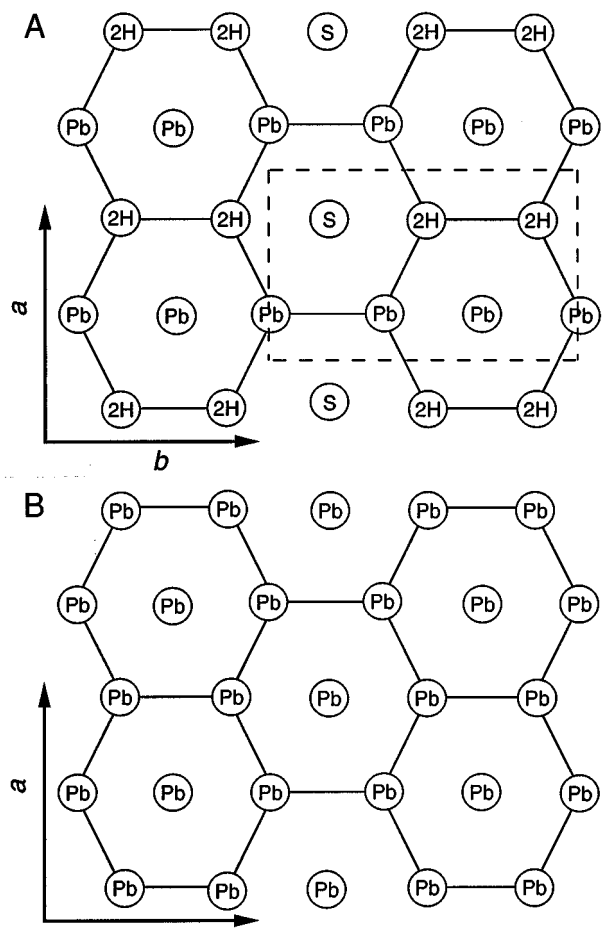

FIG. 3. Idealized cation arrays in layers A and B. Layer A includes both S and 2H replacing Pb while maintaining the hexagonal net. Layer B has the same hexagonal net but with only Pb. These two layers are stacked in the sequence ..BAABAA..

Layer A

Layer A is shown in detail in Fig. 4 and includes oxygens and hydrogen in addition to Pb. Figure 4a shows the same view as in Fig. 2 while 4b shows a plan view of the A layer parallel to [001] which can be compared to the idealized view of layer A given in Fig. 3. The Pb3 and Pb4 polyhedra form an alternating edge-sharing and face-sharing chain parallel to [010] and these chains are then cross-linked by SO_4 groups within the A layer (Fig. 4b). The two oxygens in the edge sharing each have long Pb–O distances near 2.9 Å, while the face-sharing oxygens have two (O1 and O3) short Pb–O bonds near 2.4 Å and one (O7) near 2.9 Å. The O7 oxygen forms the link with the adjacent A layer with long distances of 2.9 Å to each of the Pb3 and Pb4, suggesting weak linkage between these two adjacent A layers. The oxygens (O2 and O4) which form the link to the B layer each show short distances near 2.3 Å. All Pb–O distances where the oxygen also belongs to the SO_4 group are in the range of 2.8 to 3.2 Å, giving a weak linkage within the A layer between adjacent chains. The hydrogen atoms within a chain provide only weak links to adjacent chains by hydrogen bonding to sulfate groups. In plan (Fig. 4b), the Pb3, Pb4, SO_4, and H1–H2 form a slightly distorted hexagonal net as indicated by the dashed lines which can be compared to the idealized layer A net shown in Fig. 3. This pattern suggests that the SO_4 group and the H pair can replace the Pb atoms while maintaining this hexagonal net geometry; this net can also be recognized in the B layer as described below.

Layer B

Layer B is illustrated in Fig. 5 where Fig. 5a is the same projection as in Fig. 2 and Fig. 5b is the plan view of Layer B onto (001); both Fig. 5a and Fig. 5b include oxygen atoms as well as lead. Figure 5a shows a dense chain of joined PbO_5 and PbO_6 polyhedra with the sequence … Pb2–Pb1–Pb1–Pb2–Pb2 … and each sharing an edge. For Pb2–Pb2, the common oxygens are both O4, for Pb1–Pb1, the common oxygens are both O2, and for Pb1–Pb2, the common oxygens are O2 and O4. If the Pb2–O3 distance of 3.38 Å is considered a bond, then Pb1–Pb2 would be face-sharing polyhedra and Pb2 would be six coordinated. These chains are not linked within Layer B except indirectly by O1 and O6 which are both common with Layer A (Fig. 5b). Examination of Fig. 5b also shows that the lead atoms are in a hexagonal net as indicated by the dashed lines. This is the same pattern recognized in Layer A except for the SO_4 and H_2 substitution and can be compared with the idealized Layer B net shown in Fig. 3.

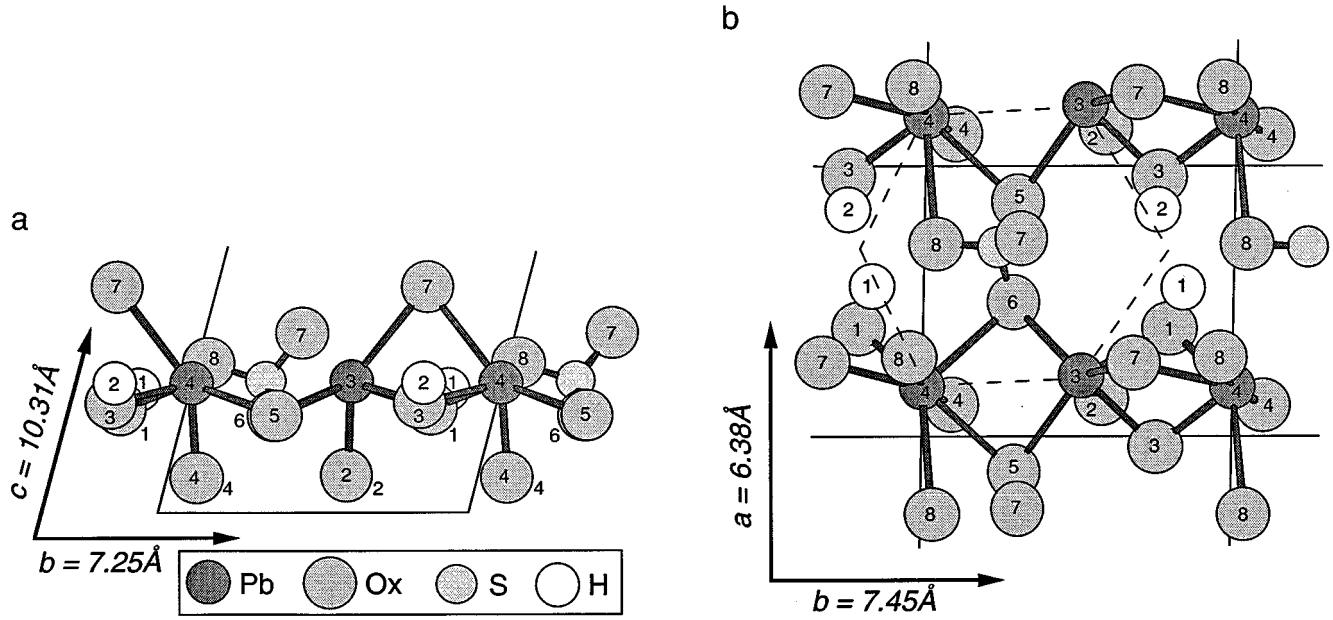

FIG. 4. (a) Projection of Layer A parallel to [100]. The sequence … Pb4–Pb3–Pb4 … can be seen where the Pb3 and Pb4 edge share O5 and O6 on the left and face share O1, O3, and O7 on the right. (b) Layer A in plan view projected onto (001). The … Pb4–Pb3–Pb4 … chains are horizontal and cross-linked by SO_4 groups. Hydrogens reside between these chains.

Hydrogen

The neutron diffraction data allowed the determination of the hydrogen positions in this structure. While the sample used for the neutron study was not the same as that for the X-ray studies, the refined atomic positions for the neutron data agree well with those for X-ray data. Using the hydrogen positions from the neutron data and the parameters for the other atoms from the X-ray data, the geometry of the hydrogen positions within tribasic lead sulfate can be

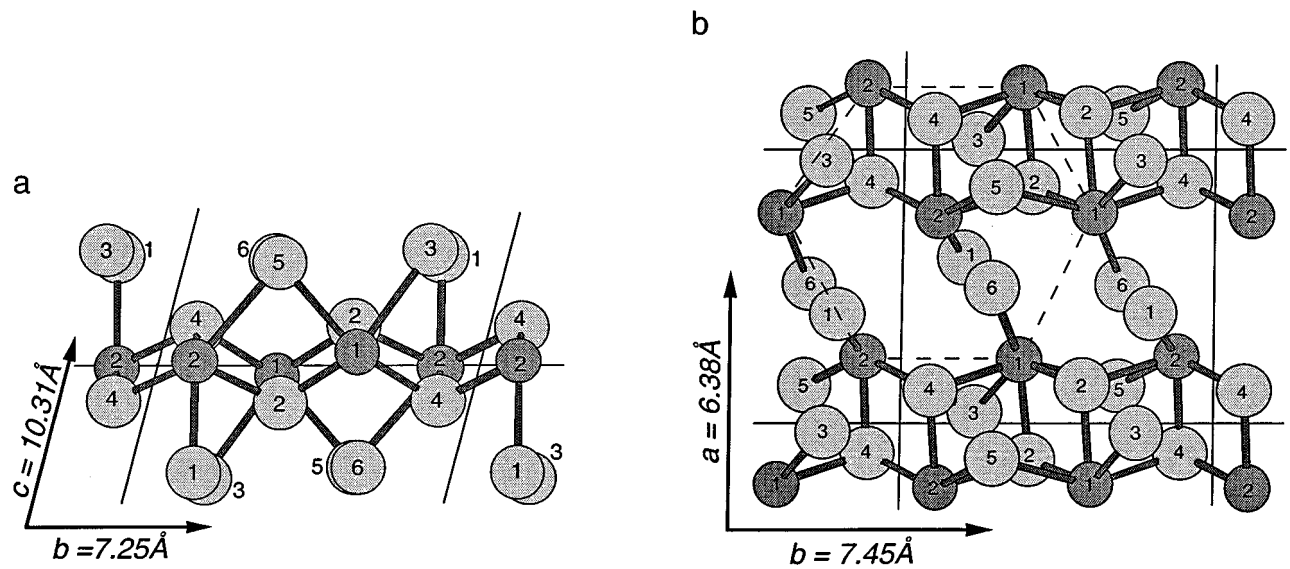

FIG. 5. (a) Projection of Layer B parallel to [100]. The sequence … Pb1–Pb1–Pb2–Pb2–Pb1 … represents a chain of edge sharing polyhedra where adjacent Pb1 polyhedra share two O2 along an edge, adjacent Pb2 polyhedra share two O4 along an edge, and the Pb1 and Pb2 polyhedra share an O2 and an O4 along an edge. (b) Layer B in plan view projected onto (001). The individual chains are clearly shown with no bonding between except for O6 and O1 through the A layers above and below this layer. The hexagonal net formed by the Pb atoms is shown by dashed lines. Atom shading as in Fig. 4.

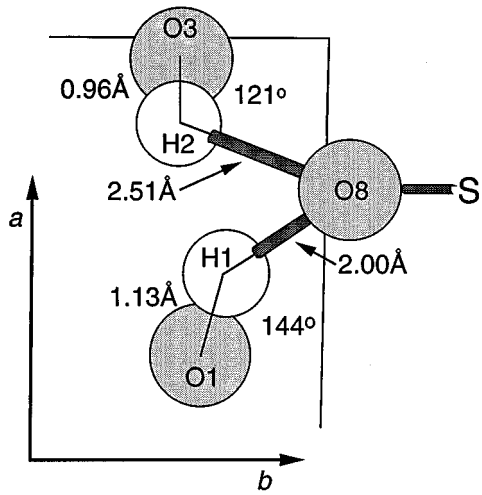

FIG. 6. Geometric details of hydrogen coordination. The two hydrogens have long bonds of 2.51 and 2.0 Å to O8, belonging to the SO_4 group. In turn the two hydrogens have much shorter bonds of 0.96 and 1.13 Å to O3 and O1, respectively, and show $\angle$O8---H2–O3 = 121° and $\angle$O8---H1–O1 = 121°. All atoms lie approximately in a plane parallel to (001).

defined. Figure 6 presents this configuration for the hydrogen atoms.

To a first approximation all coordination is in the plane parallel to (001). Both hydrogens are within hydrogen bonding distance of O8 which belongs to the SO_4 group and all are included in layer A. The hydrogen O8 distances are 2.00 and 2.51 Å, suggesting very weak bonding. The H2 and H1 hydrogens in turn are bonded to O3 and O1, respectively, with distances near 1.0 Å.

Lead Polyhedra

The lead polyhedra are far from regular and range from PbO_5 to PbO_8 but the coordination number depends on what Pb–O distance can be considered to be a bond. Bond length data in Table 6 used a maximum of 3.20 Å. Each of the four lead atoms are pictured with their coordination in Fig. 7 as viewed parallel to [100], the same view as shown in Fig. 2. Hydrogens are included in these polyhedra and all distances are indicated. For each of the four polyhedra, there are three short PbO distances ranging from 2.25 to 2.39 Å. The averages for these three for each polyhedron are 2.31, 2.31, 2.31, and 2.34 Å, respectively, for Pb1 through Pb4. The remaining Pb–O distances range from 2.63 to near 3.20 and average 2.86, 2.83, 2.86, and 3.03 Å, respectively, for Pb1 through Pb4. Each of the four polyhedra has one additional long Pb–O distance as shown in Fig. 8 but not given in Table 5 (Pb1–O6 = 3.44 Å, Pb2–O3 = 3.41 Å, Pb3–O7 = 3.51 Å, and Pb4–O8 = 3.33 Å).

TABLE 6
Bond Lengths for $3PbO \cdot PbSO_4 \cdot H_2O$ Based on X-Ray Data (Except for H)

Pb (1)–O (2)	2.296(5)	Pb (2)–O (4)	2.272(5)	Pb (3)–O (2)	2.254(5)
–O (4)	2.322(5)	–O (4)	2.329(5)	–O (1)	2.330(6)
–O (2)	2.323(5)	–O (2)	2.334(5)	–O (3)	2.356(6)
–O (5)	2.741(6)	–O (1)	2.625(6)	–O (6)	2.788(7)
–O (6)	2.863(7)	–O (5)	3.036(7)	–O (5)	2.845(6)
–O (3)	2.973(7)			–O (7)	2.953(6)
Pb (4)–O (4)	2.280(6)	H (1)–O (1)	1.126(28)	S–O (7)	1.455(7)
–O (1)	2.370(6)	–O (8)	2.000(24)	–O (8)	1.468(7)
–O (3)	2.385(6)			–O (6)	1.477(6)
–O (5)	2.921(6)			–O (5)	1.494(6)
–O (7)	2.937(7)	H (2)–O (3)	0.96(4)		
–O (6)	3.001(7)				
–O (8)	3.123(7)				
–O (8)	3.173(7)				

Oxygen Coordination

Table 7 presents the coordination of each oxygen and these can be divided into several groups based on the general Pb–O bond length and coordination environment.

Group 1: O2 and O4, which are bonded only to Pb each show four short Pb–O bonds.

Group 2: O5, O6, and O7, which are bonded to S and Pb show either three or four long Pb–O bonds.

Group 3: O1 and O3 each have one short O–H bond, two short Pb–O bonds, and either one or two long Pb–O bonds.

Group 4: O8 shows three long Pb–O bonds, coordination to S, and two long O–H bonds.

TABLE 7
Oxygen Coordination and Distance (Å)[a]

	Pb1	Pb2	Pb3	Pb4	S	H1	H2
O1	—	2.63	2.33	2.37	—	1.12	—
O2	2.30, 2.33	2.33	2.25	—	—	—	—
O3	2.97	3.41	2.36	2.39	—	—	0.96
O4	2.32	2.27, 2.33	—	2.28	—	—	—
O5	2.74	3.04	2.85	2.92	1.49	—	—
O6	2.86, 3.44	—	2.79	3.00	1.48	—	—
O7	—	—	3.51, 2.95	2.94	1.46	—	—
O8	—	—	—	3.12, 3.17, 3.33	1.47	2.00	2.51

[a] Distances given for Pb–O to 3.51 Å although not all may be considered bonding.

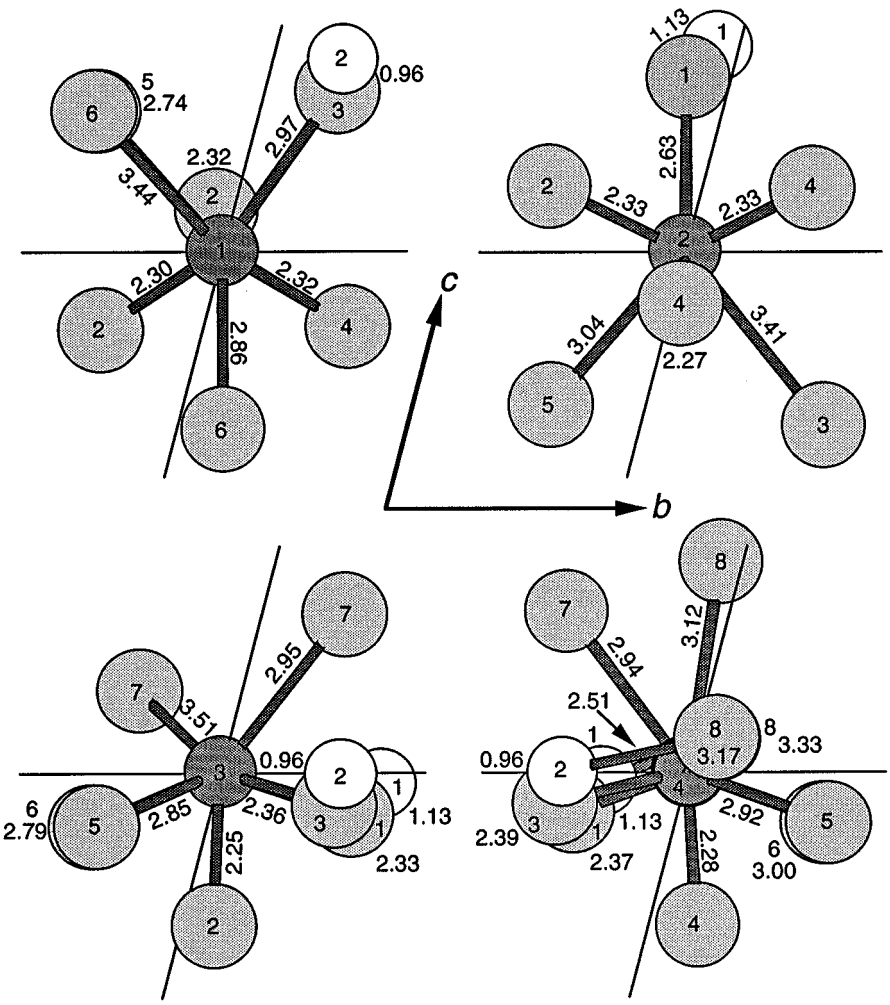

FIG. 7. Geometry of coordination polyhedra of four lead atoms. Hydrogen positions are also shown. All are drawn as projected parallel to [100]. Included are four long Pb–O bonds, Pb1–O6 = 3.44 Å, Pb2–O3 = 3.41 Å, Pb3–O7 = 3.51 Å, and Pb4–O8 = 3.33 Å. These are not given in Table 7 but are discussed in the text.

Structural Relationship between Tribasic Lead Sulfate and Two PbO Structures

Close examination of the structures of orthorhombic (7) and tetragonal (8) PbO and that of tribasic lead sulfate shows a basic structural unit common to all three. For this comparison, we consider only Pb–O distances less than 2.5 Å as these should be the strongest bonds. When only these Pb–O bonds are considered, both PbO structures appear very similar and are composed of compressed bands as shown in Figs. 8b and 8c. This unit in orthorhombic PbO shows a greater compression (shortened repeat) but otherwise is identical to the same unit in tetragonal PbO. These bands are linked by similar short bonds as shown by the vertical linkages in Figs. 8b and 8c. In tribasic lead sulfate, as illustrated in Fig. 8a, these same bands can also be recognized. In one case the band is virtually identical to that in the PbO structures, while adjacent bands preserve the same topology but with half the Pb sites replaced by equal numbers of sulfate and OH groups. Schematically this is illustrated in Fig. 8 where the unshaded atom sites in both PbO structures are replaced by sulfate and OH groups while the shaded portion of the PbO structures are preserved to form the tribasic lead sulfate structure.

The chemical formula for tribasic lead sulfate as generally written, $3PbO \cdot PbSO_4 \cdot H_2O$, may be more accurately written as $4PbO \cdot H_2SO_4$ to emphasize that H_2O is not present in the structure but rather O–H and SO_4 units substitute for Pb.

Relevance to Lead–Acid Batteries

In addition to providing a description of the tribasic lead sulfate structure, the above discussion shows a clear

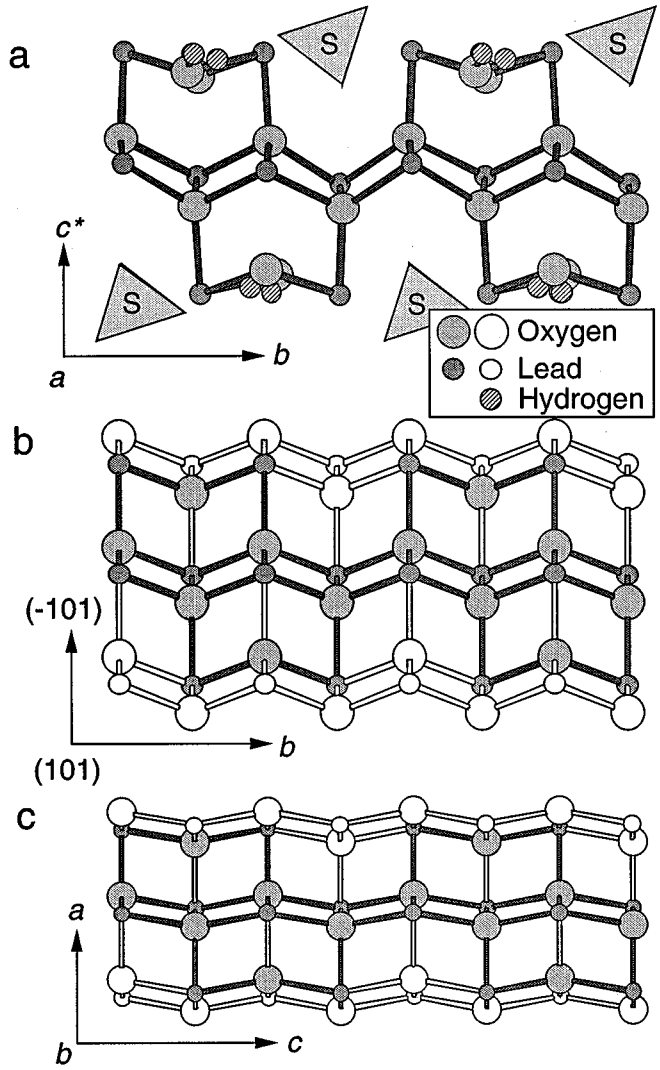

FIG. 8. Projections of (a) tribasic lead sulfate, (b) tetragonal PbO, and (c) orthorhombic PbO to illustrate structural similarities. Only Pb–O bonds of less than 2.5 Å are shown as these are considered to represent the strongest bonds and define the similar structural units in these three structures. A common structural unit is a slightly compressed band shown shaded in each structure and running left to right. Both PbO structures are composed only of these units. In tribasic lead sulfate, portions of these units (shown by open symbols in the PbO structures, are replaced by both sulfate and 2(OH) groups as illustrated in (a).

similarity between the lead oxides and this lead sulfate. During production of lead acid batteries, sulfuric acid (H_2SO_4) is added to either or both polymorphs of PbO to produce sulfates. The structural similarity strongly suggests that the reaction,

$$4PbO + H_2SO_4 \rightarrow 3PbO \cdot PbSO_4 \cdot H_2O,$$

may involve nucleation and growth on preexisting PbO. While this is certainly not proved by the structural similarity, various observations in the literature suggest that the sulfate is controlled to some extent by the polymorph of PbO present in the reactants. Both have similar structural elements, but one may favor the formation of tribasic lead sulfate over other sulfates. Dynamic neutron diffraction experiments where intermediate compounds might be identified during reaction may provide definitive mechanisms.

ACKNOWLEDGMENTS

IMS appreciates financial support from NASA NAGW-3416. J. J. P. thanks MRSEC (Grant NSF-DMR-00379) and CARS (Grants DOE FG02-94ER14466 and NSF EAR-9317772), both at the University of Chicago, for financial support. Dr. H. G. Kuzel kindly supplied the single crystals used in this study while Mr. Dale Krausnick and Mr. Frank Kusba of the Halstab Division of the Hammond Group prepared the powdered sample for neutron diffraction. Work performed at Argonne National Laboratory was supported by the U.S. Department of Energy, Basic Energy Sciences (DOE-BES) under Contract W-31-109-ENG-38.

REFERENCES

1. H. Bode, "Lead–acid Batteries," Wiley, New York, (1977).
2. I. M. Steele and J. J. Pluth, to be submitted (1997).
3. H.-J. Kuzel, *N. Jb. Miner. Mh.* **3,** 110 (1973).
4. J. D. Jorgensen, J. Faber, Jr., J. M. Carpenter, R. K. Crawford, J. R. Haumann, R. L. Hitterman, R. Kleb, G. E. Ostrowski, F. J. Rotella, and T. G. Worlton, *J. Appl. Crystallogr.* **22,** 321 (1989).
5. A. C. Larson and R. B. Von Dreele, "Generalized Crystal Structure Analysis System," Los Alamos National Laboratory, LAUR 86-748, 1986.
6. K. Sahl, *Zeit. Kristallogr.* **132,** 99 (1970).
7. M. I. Kay, *Acta Crystallogr.* **14,** 80 (1961).
8. J. Leciejewicz, *Acta Crystallogr.* **14,** 1304 (1961).